

Conductivity and Dielectric Studies of $\text{Li}_2\text{ZnSiO}_4$ Ceramic Electrolyte Synthesized via Citrate Sol Gel Method

S.B.R.S Adnan^{1,*} and N.S. Mohamed²

¹Institute of Graduate Studies, University of Malaya, 50603 Kuala Lumpur, Malaysia

²Centre for Foundation Studies in Science, University of Malaya, 50603 Kuala Lumpur, Malaysia

*E-mail: syed_bahari@yahoo.com

Received: 30 July 2012 / Accepted: 6 September 2012 / Published: 1 October 2012

Lithium zinc silicate ceramic powders have been synthesized by a sol gel method. The formation of the compound has been confirmed by X-ray diffraction and energy dispersive X-ray. The conductivity of the material increases linearly with temperature. The sample sintered at 850°C show highest dc conductivity with $5.00 \times 10^{-6} \text{ S cm}^{-1}$ at room temperature and increase to $5.54 \times 10^{-4} \text{ S cm}^{-1}$ at 500°C respectively. The frequency dependence of conductivity obeys the universal power law variation, $\sigma'(\omega) = \sigma(0) + A\omega^n$. The plot of pre-exponent n versus temperature suggests that the conduction mechanism in the system can be described using correlated barrier hopping model. Several important parameters such as mobile ion density and ionic mobility have been determined. The increasing trend of these parameters as well as the results of dielectric study indicates that the increase in conductivity with temperature is due to increase in mobility of mobile ions with temperature.

Keywords: Arrhenius, ceramic, dielectrics, electrolyte, Lisicon.

1. INTRODUCTION

In the search for new ion conducting crystalline materials, ceramic electrolytes form an important class of materials. This type of electrolyte materials offers advantages such as large electrochemical stability window, good thermal stability, important safety asset, absent of leakage and a high resistance to shock and vibrations [1].

Ceramics electrolytes are the only solid electrolytes that have ordered structure. They basically consist of mobile ions in less or more rigid crystalline frameworks. The ionic conduction in the crystalline electrolytes is through 1D, 2D or 3D channels depending on the crystal structure [2]. Good

ionic conduction is the key requirement for the solid electrolyte to minimize cell impedance also has little or no electronic conduction to minimize leakage currents [3].

Ionic conduction in this type of electrolytes occurs by movement of ionic point defects which requires energy in their periodic lattice structure. These point defects produce interstitial or vacancy ions. Increasing temperature will increase their ionic conductivity. Thus, crystalline solid electrolytes are well suited for high temperature application. However, ionic conduction in some compounds is reasonably high even at relatively low temperature. As such, several types of ion conducting inorganic crystalline materials have also been investigated for use in electrochemical devices operating at low and elevated temperature [4].

$\text{Li}_2\text{ZnSiO}_4$ one of the promising ceramic electrolytes, is categorized into LISICON (Lithium Super Ionic Conductor) type. This type is based on γ -tetrahedral structures, Li_2MXO_4 , ($\text{M} = \text{Zn, Mg, Ca}$), ($\text{X} = \text{Ge, Si, Ti}$) which is isostructural with $\gamma\text{-Li}_3\text{PO}_4$ [5-8]. The LISICON structure is consisted of hexagonal close packed oxygen ion arrays where the cations occupy half of the tetrahedral site. The lithium ion diffusion is expected to occur through tetrahedral site and interstitial octahedral site pathway [9-10]. This indicates that the lithium ion distribution between tetrahedral site and interstitial octahedral site are important factors to create lithium ion conduction pathway that affects their ionic conduction [11-18].

The most common method used to prepare $\text{Li}_2\text{ZnSiO}_4$ ceramic materials is solid state reaction technique. However, this method commonly leads to many problems such as the use of high firing temperature (usually $>1000^\circ\text{C}$) for a prolonged period (1-2 days), contamination with impurities, volatilization, lack of control of microstructure and composition and suffer from obtaining good materials free of grain boundary resistance [19].

In recent years, considerable research has been done on the synthesis of advanced ceramic materials using the sol gel technique. Compare to the conventional methods, the most attractive features and advantages of sol-gel process include (a) molecular-level homogeneity can be easily achieved (b) the homogeneous mixture containing all the compounds in the correct stoichiometry ensures a much higher purity; and, (c) much lower heat treatment temperature to form glass or polycrystalline ceramics is usually achieved without resorting to a high temperature [20-21].

In this study, $\text{Li}_2\text{ZnSiO}_4$ compounds were prepared via sol gel method. Detail study on their conductivity and dielectric properties were carried out since such study on this compounds using this method has never been reported in the literature.

2. EXPERIMENTAL PROCEDURE

2.1. Synthesis of $\text{Li}_2\text{ZnSiO}_4$

Lithium acetate ($\text{C}_2\text{H}_3\text{LiO}_2$) zinc acetate ($\text{C}_4\text{H}_{10}\text{O}_6\text{Zn}$) and tetraethyl orthosilicate ($\text{SiC}_8\text{H}_{20}\text{O}_4$) were used as the starting materials while citric acid was used as the chelating agent. $\text{C}_2\text{H}_3\text{LiO}_2$ and $\text{C}_4\text{H}_{10}\text{O}_6\text{Zn}$ were first dissolved in distilled water before mixing with citric acid under magnetic stirring. The solution was transferred into a reflux system and continuously stirred until a

homogeneous solution was formed. Solution of $\text{SiC}_8\text{H}_{20}\text{O}_4$ was later added to this homogeneous solution and stirred for 12 hours. The solution was taken out and then vaporized for about 2 hours under magnetic stirring at 75°C . The resulting wet gel was dried in a vacuum oven at 150°C for 24 hours to remove water particles, resistance organic groups and also to avoid ceramic cracks. The obtained powder was ball milled for 1 hour using a Fritsch Pulverisette-7 which was operated at 300 rpm. The powder was pressed using a Specac pellet press to form pellet which was later sintered at different temperature for 12 hours.

2.2. Characterization techniques.

X-ray diffraction (XRD) was performed in order to elucidate structural information of the sample. The sintered ceramic powders were characterized using a Bruker AXS D8 Advance X-ray Diffraction spectrometer with Cu-K_α radiation of wavelength of 1.5406 \AA in 2θ range between 10° to 70° . The morphology of the samples was observed by the Scanning Electron Microscopy (SEM) while Energy Dispersive Xray (EDX) technique was employed for elemental analysis.

The ceramic electrical properties were determined by ac impedance spectroscopy using Solatron 1260 impedance analyzer over a frequency range from 0.1 to 10^6 Hz. An applied voltage was fixed at 110 mV. The dc conductivity was determined using the equation:

$$\sigma_b = \frac{d}{AR_b} \quad (1)$$

where d is the sample thickness, A is the area of the electrode and R_b is the bulk resistance.

The value of the dielectric constant (ϵ') and dielectric loss (ϵ'') of $\text{Li}_2\text{ZnSiO}_4$ were calculated using the formula:

$$\epsilon' = \frac{Z''}{\omega C_o(Z'^2 + Z''^2)} \quad (2)$$

and

$$\epsilon'' = \frac{Z'}{\omega C_o(Z''^2 + Z'^2)} \quad (3)$$

where Z' and Z'' are the real and imaginary impedances obtained from impedance measurements, ω is $2\pi f$ and $C_o = \epsilon_o A/d$ (ϵ_o : the permittivity of the free space ($8.854 \times 10^{-14} \text{ F cm}^{-1}$ and A : area of electrode).

The ac currents (I) can be separated into charging current ($i\omega\epsilon'$) C_oV and loss current ($\omega\epsilon''$) C_oV as given by the following equation,

$$I = (i\omega\epsilon' + \omega\epsilon'')C_oV \quad (4)$$

By using the relation $C_o = \epsilon_o A/d$, the current density (J) can be related to the complex admittance (Y^*) as follows,

$$J = (i\omega\epsilon' + \omega\epsilon'')E = (i\sigma'' + \sigma')E = Y^*E \quad (5)$$

Therefore,

$$\sigma' = \omega\epsilon_o\epsilon'' \text{ and } \sigma'' = \omega\epsilon_o\epsilon', \quad (6)$$

where σ' is loss current conductivity (conductance), also known as ac conductivity σ_{ac} in the present study, and σ'' is the conductivity due to charging current (susceptance). On the other hand, complex admittance (Y^*) is the inverse of Z^* .

The ac conductivity has been evaluated from dielectric data in accordance with the relation:

$$\sigma_{ac} = \omega\epsilon_o\epsilon'' \tan \delta$$

where ϵ_o is permittivity of the free space, ω is $2\pi f$ and $\tan \delta$ is the dielectric loss factor [22].

3. RESULT AND DISCUSSION

3.1. Phase Identifications

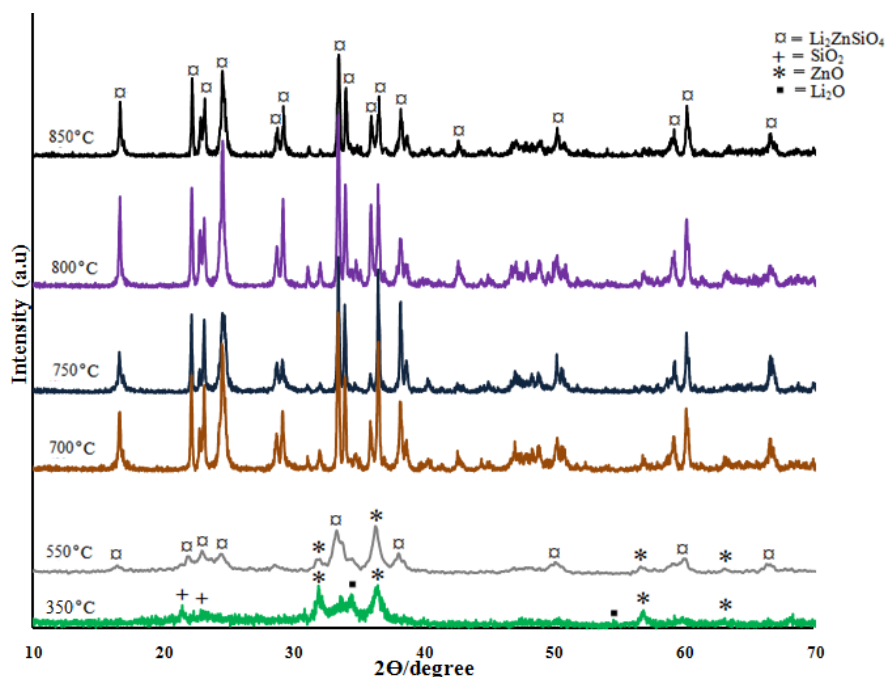


Figure . 1 : XRD pattern of samples sintered at different temperature.

Presented in Fig. 1 are the XRD spectra of $\text{Li}_2\text{ZnSiO}_4$ sintered at different temperatures for 12 hours. As can be seen in the figure, sintering at 350°C did not successfully produce $\text{Li}_2\text{ZnSiO}_4$ compound. However the samples sintered at 550°C exhibits diffraction peaks which is attributed to $\text{Li}_2\text{ZnSiO}_4$ and ZnO , indicating the presence of impurities in the sample. The XRD spectrum of the samples sintered at temperature 700°C to 850°C shows peak attributed only to $\text{Li}_2\text{ZnSiO}_4$ showing that pure $\text{Li}_2\text{ZnSiO}_4$ has been obtained.

The pure $\text{Li}_2\text{ZnSiO}_4$ compound is found to be single phase in nature, crystallizing in monoclinic structure with space group $P2_1/m$ and lattice parameters are $a = 6.253\text{\AA}$, $b = 10.685\text{\AA}$, $c = 4.929\text{\AA}$ and $\beta = 90^\circ$ [23].

3.2. SEM and EDX analysis

Fig. 2 presents SEM micrographs and EDX spectra of the $\text{Li}_2\text{ZnSiO}_4$ ceramic powder sintered at 700°C , 750°C , 800°C and 850°C . From these images, it is clear that the average grain size decreases with increase in sintering temperature; from $2\ \mu\text{m}$ in the sample sintered at 700°C to $0.1\ \mu\text{m}$ in the sample sintered at 850°C . In order to confirm the stoichiometric proportions, the EDX analysis was performed. This analysis was carried out at larger region (marked as A) to measure the average composition and smaller region (marked as B) to show whether the composition of A is homogeneous on a relatively small scale. The atomic ratios of Zn and Si was calculated and listed in Table 1. The result shows that the atomic ratios in both region A and region B for Zn: Si are homogeneous.

The EDX of the sample could not display the presence of lithium because of its light weight [24]. As such, the concept of charge neutrality was employed [25]. It is found that, the ratio of $\text{Li} : \text{Zn} : \text{Si} = 2.0 : 1.0 : 1.0$ confirming the formation of $\text{Li}_2\text{ZnSiO}_4$ compound.

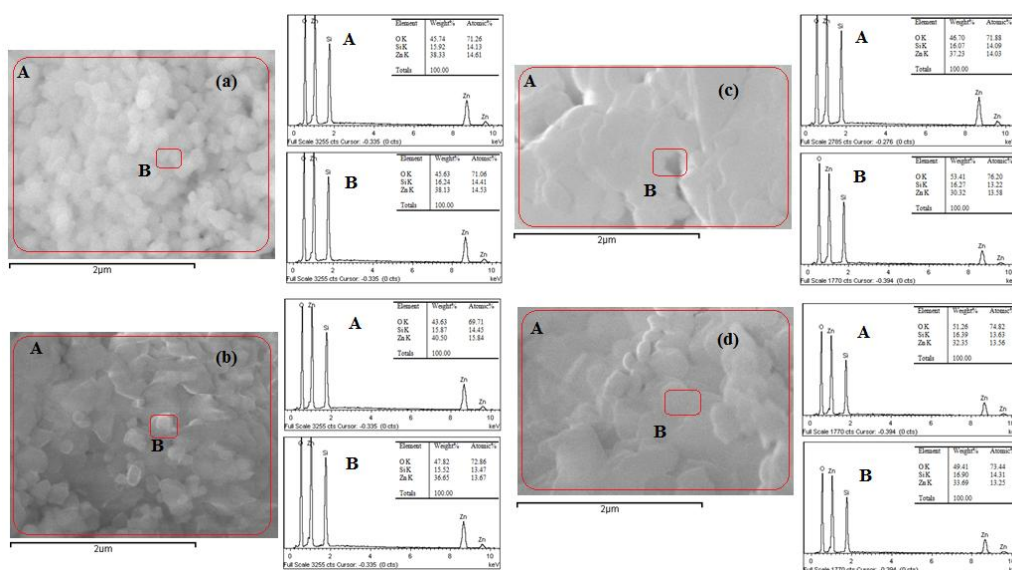


Figure 2. SEM micrographs (left) and EDX analysis (right) of the $\text{Li}_2\text{ZnSiO}_4$ ceramics powder sintered at (a) 850°C (b) 800°C (c) 750°C and (d) 700°C

Table 1. The atomic ratios of Zn and Si for the sample sintered at different temperature

Sample	Atomic Ratio			
	Region A		Region B	
	Zn	Si	Zn	Si
850°C	1	0.9671	1	0.9917
800°C	1	0.9122	1	0.9833
750°C	0.9957	1	1	0.9734
700°C	0.9949	1	0.9259	1

3.4. Conductivity Measurement

3.4.1. Direct current conductivity

The dc conductivity of $\text{Li}_2\text{ZnSiO}_4$ ceramic solid electrolyte has been determined from the bulk resistance, R_b using equation (1). The dc conductivity for samples sintered at 700°C, 750°C, 800°C and 850°C at 500°C and RT are listed in Table 2.

Table 2. Conductivity data for $\text{Li}_2\text{ZnSiO}_4$ at RT and 500°C for all samples

Samples	σ_{500} (S cm^{-1})	σ_{RT} (S cm^{-1})
700°C	4.74×10^{-5}	1.81×10^{-7}
750°C	1.08×10^{-4}	5.82×10^{-7}
800°C	3.03×10^{-4}	1.13×10^{-6}
850°C	5.54×10^{-4}	5.80×10^{-6}

In order to confirm the conductivity obtained from the impedance plots, conductivity spectra (imaginary part of conductivity, σ'' versus real part of conductivity, σ') are plotted and typical spectra recorded at RT are shown in Figure 3. The conductivity plots consists of a semicircle and two dispersion curves at low σ' and high σ' regions, respectively. The intercept of the dispersion curves with x-axis at high gives the value of bulk conductivity, σ_b . This method has been used by a few groups of researchers [26-31]. Table 3 lists the dc conductivity values obtained from the conductivity spectra. It is observed that the values of dc conductivity obtained from both conductivity spectra and impedance at RT are close to each other hence confirming the value of dc conductivity obtained from the impedance plots.

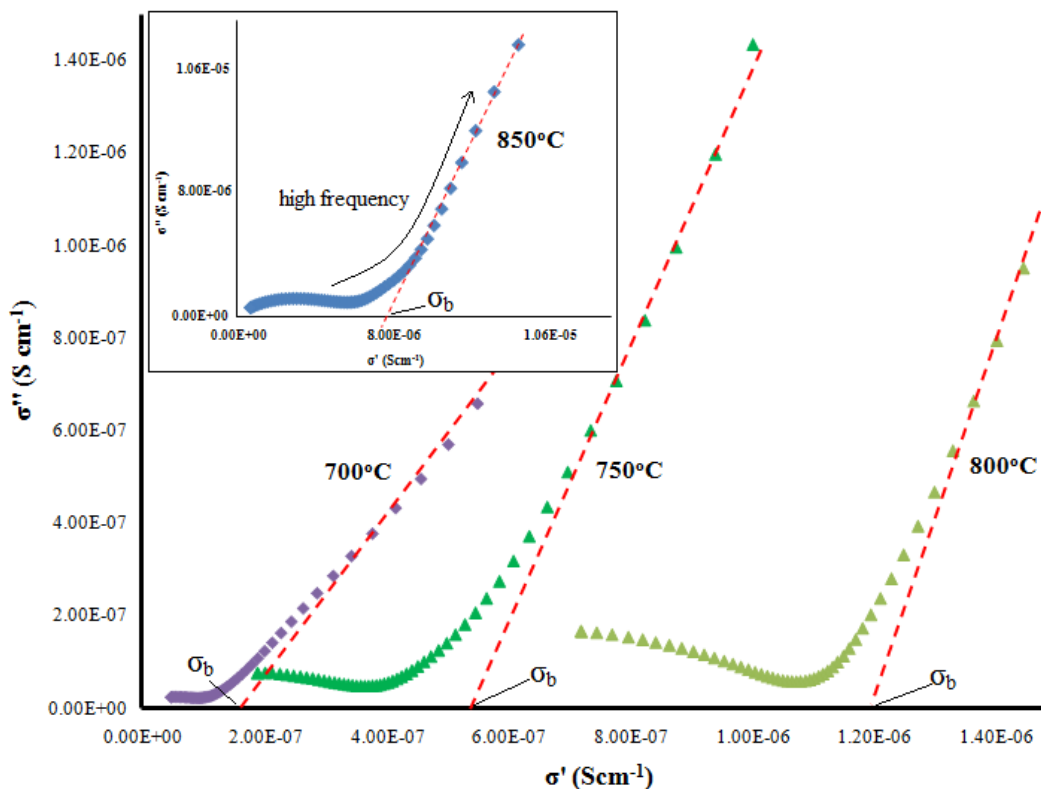


Figure 3. Conductivity plot of $\text{Li}_2\text{ZnSiO}_4$ sintered at various temperatures.

Table 3. Comparison of conductivity values determined from impedance and conductivity plots for all samples

Samples	Z plot (S cm^{-1})	σ plot (S cm^{-1})
	σ_{bulk}	σ_{bulk}
700°C	1.81×10^{-7}	1.85×10^{-7}
750°C	5.82×10^{-7}	5.86×10^{-7}
800°C	1.13×10^{-6}	1.15×10^{-6}
850°C	5.80×10^{-6}	5.82×10^{-6}

The increase in dc conductivity with temperature is influenced by thermally activated drift mobility of ions. The activation energy for the thermally activated hopping process was obtained by fitting the dc conductivity data with Arrhenius equation:

$$\sigma_b T = A \exp\left(\frac{-E_a}{kT}\right) \quad (8)$$

where A is the pre-exponential factor, E_a is the activation energy for conduction and k is the gas constant. Figure 4 depicts the Arrhenius plot for the samples sintered at 700°C, 750°C, 800°C and 850°C. The sample sintered at 700°C, 750°C and 800°C shows linear plot suggesting that there are no

structure and phase changes in the sample for the studied temperature range [32] . However, for the sample sintered at 850°C, two linear regions are seen with sudden change in slope at 300°C (1000/T = 1.75 K⁻¹). The change in slope could be due to phase transition occurring in the sample upon heating [33]. The activation energy for all samples were extracted from the Arrhenius plots and are shown in Fig. 4. The low value of activation energy indicates high mobility of ions in the sample.

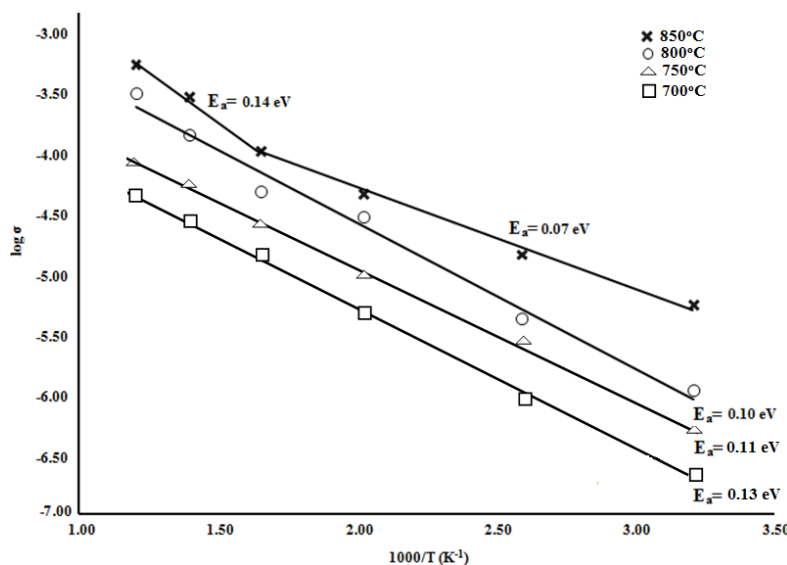


Figure 4. Arrhenius plot of the dc conductivity for Li₂ZnSiO₄ sample sintered at 700°C , 750°C, 800°C and 850°C.

3.4.2. Alternating current conductivity

Fig. 5 depicts the graph of log σ(ω) versus log ω for Li₂ZnSiO₄ sample sintered at 850°C. From the figure, it is clear that there is a plateau at low frequency region and extrapolating it to the y-axis gives the value of d.c conductivity. At the plateau region, the conductivity is frequency independent and the σ_{dc} values are found to be in good agreement with the value listed in Table 2.

The transition from the d.c plateau to a.c conductivity dispersion region shifts towards higher frequency range when temperature increases. The high frequency dispersion is due to the high probability for the correlated forward backward hopping at high frequencies together with the relaxation of the dynamic cage potential. Therefore we can say that the a.c conductivity is dominant in high frequency region [34].

The conductivity behavior obeys the universal power law :

$$\sigma'(\omega) = \sigma(0) + A\omega^n \tag{9}$$

where σ(0) is the d.c conductivity of the sample, A is a temperature dependant parameter and n is the power law exponent which represents the degree of interaction between the mobile ion and is less than 1. The value of n is extracted from the slope log σ(ω) versus log ω. The parameter of n

obtained varies from 0.68 at RT and decreases to 0.10 at the highest temperature of 773K. The plot of variation of n with temperature is illustrated in Fig. 6. The plot can also be fitted to equations $n = -0.0012x + 1.0644$. This equation suggests that $n \rightarrow 1$ when $T \rightarrow 0$.

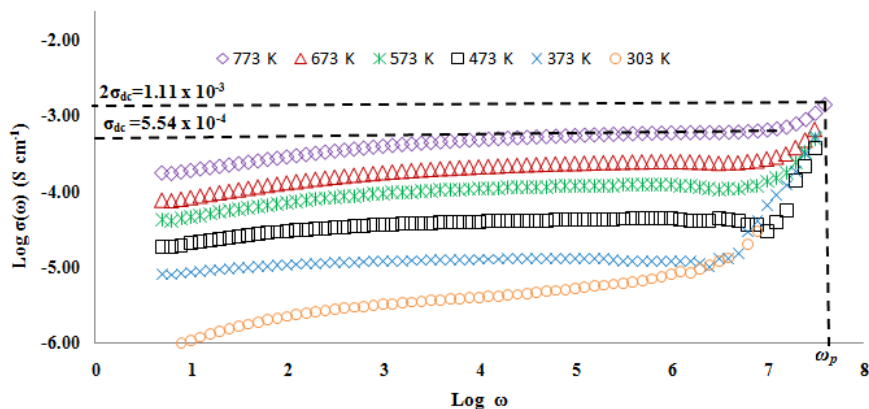


Figure 5: Log $\sigma(\omega)$ total versus log ω for $\text{Li}_2\text{ZnSiO}_4$ sample sintered at 850°C at various temperatures.

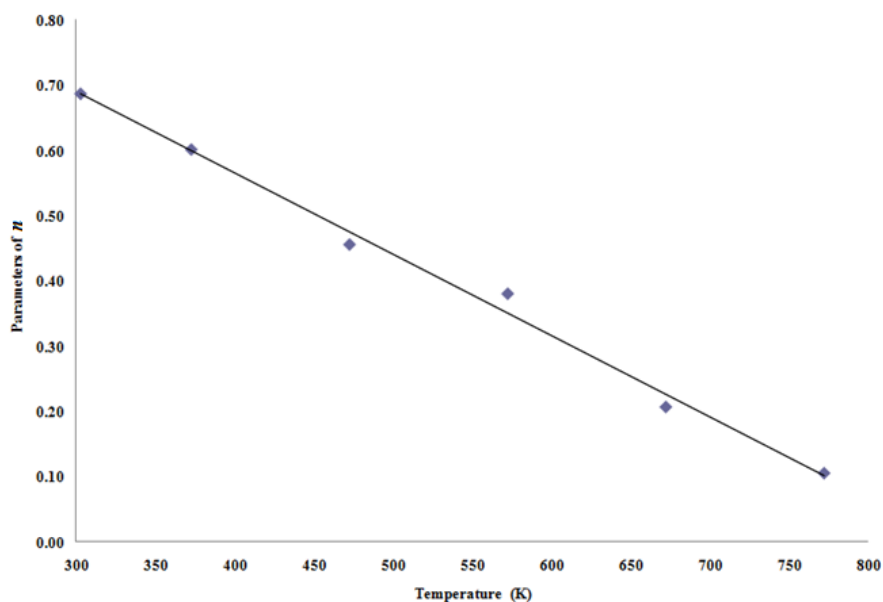


Figure 6: Value of n for $\text{Li}_2\text{ZnSiO}_4$ material at different temperature.

According to the correlated barrier hopping (CBH) model, values of n decrease with increasing temperatures and can be evaluated as follows

$$1 - n = \frac{6kT}{Wm} \tag{10}$$

where k is Boltzmann's constant, T is the temperature and W_M is the maximum barrier height. From equation (8), it can be deduced that $n \rightarrow 1$ if $T \rightarrow 0$. This confirms that the conduction mechanism in the $\text{Li}_2\text{ZnSiO}_4$ system studied can be described using the CBH model.

In this model it is assumed that the ions or charge carriers are surrounded by several potentials, such as the Coulombic repulsive potential between the ions and a potential well in which the ions reside. Superposition of the potentials yields a single ion potential that is actually felt by the ions. When the ion gains sufficient energy, they hop from one site to another. As the temperature increases, the number of ions that hop from one site to another increases, leading to an enhancement in conductivity with temperature, as observed in Fig .5 [35-36]

According to Almond and co-researchers the a.c conductivity data can also be used to estimate the ionic hopping rate, ω_p . The hopping rate of ion in a material is a valuable information to elucidate the ionic conduction. The ω_p can be obtained from the graph $\log \sigma(\omega)$ versus $\log \omega$ by extrapolating at twice the value of d.c. conductivity from the vertical axis horizontally towards the graph and then extrapolating downwards vertically to the horizontal axis as shown in Fig. 5. The magnitude of the charge carrier concentration can be obtained using the equation [34,37-39]:

$$K = \frac{\sigma T}{\omega_p} \quad (11)$$

where

$$K = ne^2 a^2 \gamma k^{-1} \quad (12)$$

Here e is electron charge, γ is correlation factor which is set equal to 1, and a is the jump distance between two adjacent sites for the ions to hope which is assumed to be 3\AA for al materials [34, 38]. n is the density of mobile ions (charge carrier) which can be calculated using eq. 10 and k is Boltzmann constant. The ionic mobility, μ can be calculated using equation:

$$\mu = \frac{\sigma_{dc}}{ne} \quad (13)$$

The value of σ , ω_p , K , n , and μ , at all temperatures studied for $\text{Li}_2\text{ZnSiO}_4$ sample sintered at 850°C are tabulated in Table 4. From the table, the mobile ion concentration, K and density of mobile ion, n are found to be constant over the temperature range studied. This reveals that all the ions which are responsible for the conductivity are in a mobile state, thus can be best represented by the strong electrolyte model [34,37]. Hence, the conduction mechanism in the investigated $\text{Li}_2\text{ZnSiO}_4$ is attributed to the hopping of charge carriers. Meanwhile, from the table the mobility of ions, μ increases with increasing temperature. This means that the increase in conductivity in the samples can be attributed to the increase in ionic mobility since the density of mobile ions is constant over temperature range studied [34,37].

Table 4. Parameters of σ , ω_p , K , n and μ at various temperature for $\text{Li}_2\text{ZnSiO}_4$ sample sintered at 850°C

T (k)	σ (S cm^{-1})	ω_p (kHz)	K ($\text{S cm}^{-1} \text{K Hz}^{-1}$)	$n \times 10^{25}$ (cm^{-3})	μ ($\text{cm}^2 \text{V}^{-1} \text{s}^{-1}$)
303	5.80×10^{-6}	212	8.28×10^{-9}	5.12	7.04×10^{-13}
373	1.50×10^{-5}	680	8.22×10^{-9}	4.91	1.90×10^{-12}
473	4.74×10^{-5}	2709	8.28×10^{-9}	4.95	5.96×10^{-12}
573	1.08×10^{-4}	7508	8.24×10^{-9}	4.93	1.36×10^{-11}
673	3.03×10^{-4}	24,818	8.22×10^{-9}	4.92	3.82×10^{-11}
773	5.54×10^{-4}	51,622	8.29×10^{-9}	4.96	6.95×10^{-11}

3.5. Dielectric behavior

The plots of frequency dependence of the dielectric constant, ϵ' and dielectric loss, ϵ'' of $\text{Li}_2\text{ZnSiO}_4$ ceramic powder sintered at different temperatures were plotted (Fig. 7 and Fig. 8) in order to obtain further information on the ion dynamic properties in this material.

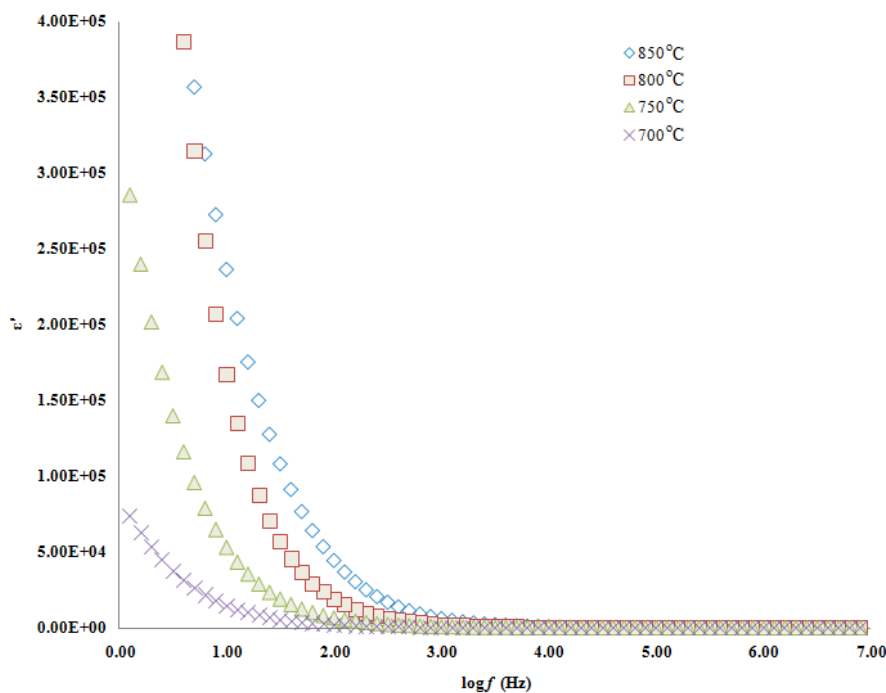


Figure 7. Plot of relative dielectric constant (ϵ') of $\text{Li}_2\text{ZnSiO}_4$ as a function of $\log f$ at different temperatures

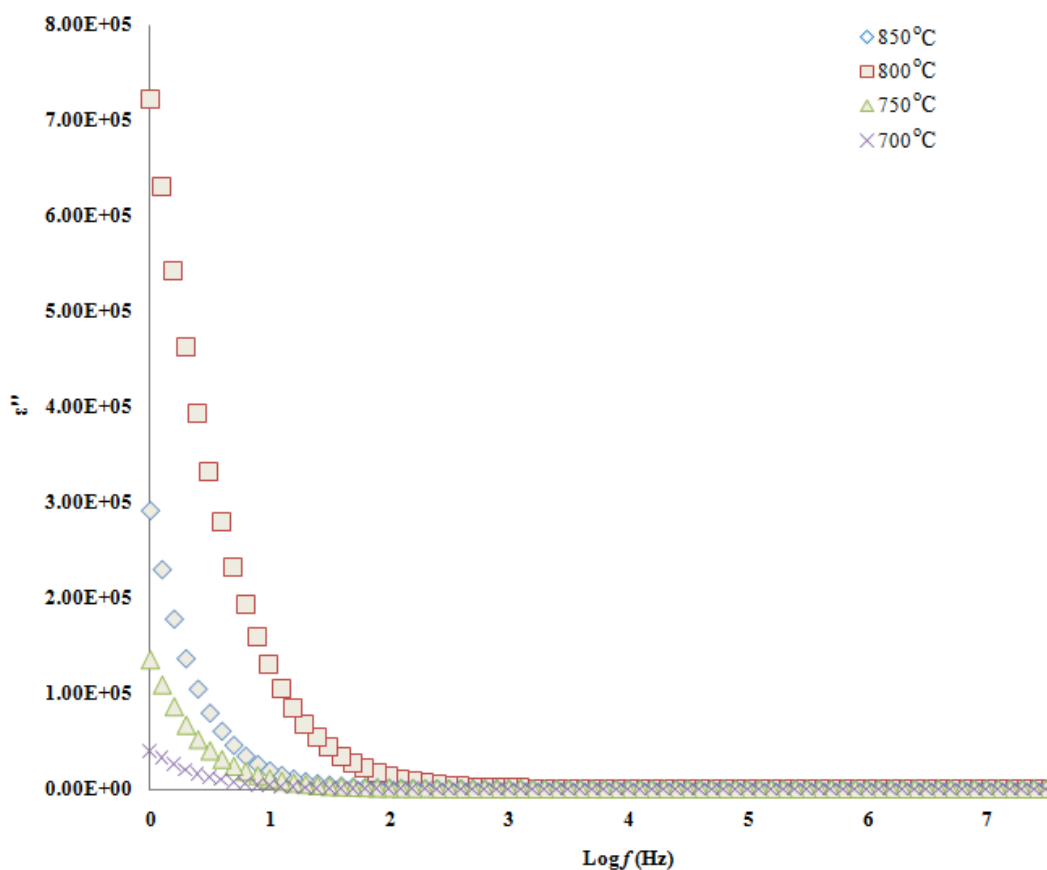


Figure 8. Plot of relative dielectric constant (ϵ'') of $\text{Li}_2\text{ZnSiO}_4$ as a function of $\log f$ at different temperatures

From both figures we can see that the dielectric constant, ϵ' and dielectric loss, ϵ'' decrease to a constant value at high frequency. At low frequencies, the high value of dielectric constant, ϵ' is attributed to the contribution of charge carrier accumulation at the interface of electrode and $\text{Li}_2\text{ZnSiO}_4$ material. Meanwhile the high value of dielectric loss, ϵ'' at these frequencies is attributed to the fact that, at low frequencies the electrical energy loss is high due to the migration of ions in the material. As the ion moves, they loss some of their energy to the lattice as heat [40-41].

However, at high frequencies, the dielectric constant, ϵ' and dielectric loss, ϵ'' value is low. This is due to high periodic reversal of the field and due to the limitation of dielectric loss sources (ion vibration only) respectively [42]. The ϵ' and ϵ'' increase with temperature indicating the fact that when the temperature is increased, the bound charge carriers get sufficient excitation thermal energy to be able to obey the charge in external field more easily. This in turn increases their contribution to the polarization resulting in increase in ϵ' and ϵ'' [40-44].

Fig. 9 presents the plot of frequency dependence of $\tan \delta$ at various temperatures. The plot shows a peaking behavior for all temperatures. As the temperature increases, the $\tan \delta$ peaks are shifted towards higher frequency. This peak is expected when the hopping frequency of ions is approximately equal to the external applied electric field. In this case

$$\omega\tau = 1 \tag{14}$$

where τ is the relaxation time of the hopping process and ω is the angular frequency of the external field ($\omega = 2\pi f_{\max}$). The relaxation time τ is inversely proportional to the jumping probability per unit time, P , according to the relation [38-39]

$$\tau = \frac{1}{2}P \quad (15)$$

so, from Eqs. (14) and (15), it is expected that f_{\max} is proportional to P . The shift of the peak of the $\tan \delta$ towards high frequency with increasing temperature, indicates that the jumping probability per unit time increases with temperature [40-41]. This result is consistent with the result discussed earlier.

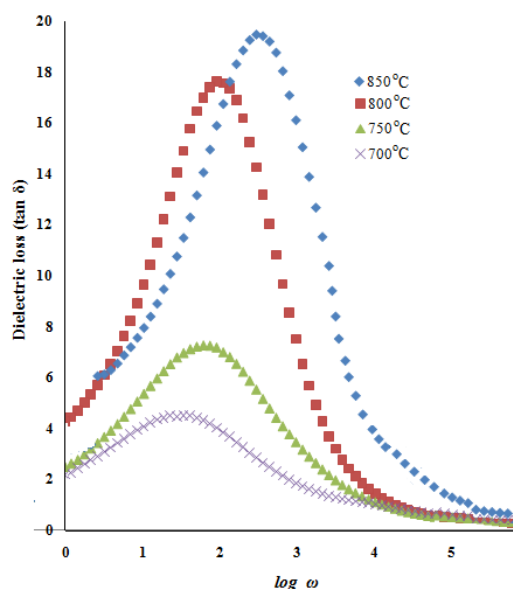


Figure 9: Frequency dependence of $\tan \delta$ at various temperatures

4. CONCLUSIONS

$\text{Li}_2\text{ZnSiO}_4$ samples have been successfully synthesized using a simple sol gel method. The XRD and EDAX analysis confirm the formation of the compound. The conductivity–temperature study shows that the compound obeys the Arrhenius law. Conductivity and dielectric studies show that the increase in conductivity with temperature is due to increase in ion mobility.

ACKNOWLEDGMENTS

Financial support by University of Malaya (PV-027/2012A) is gratefully acknowledged.

References

1. S. Tamura, A. Mori, and N. Imanaka, *Solid State Ionics*, 175 (2004) 467
2. J. W. Fergus, *J. Power Sources*, 160 (2006) 30

3. C. J Leo, Chowdari, Rao and Souquet, *Mater. Res. Bull.*, 37 (2002) 1419
4. J. W. Fergus, *J. Power Sources*, 195 (2010) 4554
5. M.A.K.L Dissanayake, H.H Sumathipala, A.R West, *Solid State Ionics*, 86 (1996) 719
6. M.A.K.L Dissanayake, P.R Gunawardane, A.R West, *Solid State Ionics*, 62 (1993) 217
7. P.G Bruce, I. Abraham, *Solid state Ionics*, 40/41 (1990) 293
8. A.D Robertson, A.R West, *Solid State Ionics*, 58 (1992) 351
9. M. Saiful Islam, (2010) *Phil. Trans. R. Soc. A*, 368 (2010) 3255
10. N.A.W Holzwarth, Yaujun A. Du, *J. Electrochem. Soc.*, 154 (2007) A999
11. M. Murayama, R. Kanno, Y. Kawamoto, T. Kamiyama, *Solid State Ionics*, 154-155 (2002) 789
12. P.G. Bruce, I. Abraham, *J. Solid State Chem.* 95 (1991) 74
13. K. Ryoji, M. Murayama, M. Irie, W. Shinya Ito, T. Hata, N. Sonoyama, Y. Kawamoto, *J. Solid State Chem.*, 168 (2002) 140
14. K. Ryoji, K. Homma, M. Yonemura, T. Kobayashi, M. Nagao, M. Hirayama (2001) *Solid State Ionics*, 182 (2001) 53.
15. A.R West, P.F. Glasser, *Solid State Chemistry*, 4 (1972) 20
16. S. Zhang, C. Deng, B.L Fu, S.Y Yang, L. Ma, *J. Electroanal. Chem.*, 644 (2010) 150.
17. C. Deng, S. Zhang, B.L Fu, S.Y. Yang, L. Ma, *Electrochimica Acta*, 55 (2010) 8482.
18. A.D Robertson, A.R. West, A.G. Ritchi, *Solid State Ionics*, 104 (1997) 1.
19. S.B.R.S Adnan, N.S Mohamed, K.A Norwati, *World Academy of Science, Engineering and Technology*, 74 (2011) 676.
20. X. Song, M. Jia, R. Chen, *J. Mater. Processing Technol.*, 120 (2002) 21.
21. R. Adnan, N.A Razana, I.A Rahman and M. Akhyar Farrukh, (2010) *J. Chinese Chem. Soc.* 57 (2010) 222.
22. H. Yamamura, S. Takeda, K. Kakinuma, *J. Chem. Soc. Jpn.* 115 (2007) 264.
23. H. Yamaguchi, K. Akatsuka and M. Setoguchi, *Acta Crystallographica Section B*, B35 (1979) 2678.
24. B.J Hwang, R Santhanam, D.G Liv, *J. Power Sources*, 97-98 (2001) 443.
25. R. Ramaraghavulu, S. Buddhudu, *Ceramics International*, 37 (2011) 3651.
26. A. Aboulaich, D.E Conte, J. Olivier-Fourcade, C. Jordy, P. Willmann, J.C. Jumas, *J. Power Sources*, 195 (2010) 3316.
27. A.F Orliukas, A. Dindune and Z. Kanape, *Electrochem. Acta*, 51 (2006) 6194.
28. R. Sobiestianskas, A. Dindune and Z. Kanape, *Mater. Sci. Engin. B*, 76 (2000) 184.
29. M. Cretin and P. Fabry, *J. European Ceramic Soc.*, 19 (1999) 2931
30. M. Godichemier, B. Micheal and Orliukas, *J. Mater. Res.* 9 (1994) 1228.
31. R. Norhaniza, R H Y Subban and N S Mohamed, *J. Mater Sci.* 46 (2011) 7815.
32. X. Wu, Z. Wen, X. Xu, X. Wang, and J. Lin, *J. Nucl. Mater.*, 39 (2009) 471.
33. K.R Koteswara, G. Rambabu, M. Raghavender, G. Prasad, G.S Kumar and M. Vithal, *Solid State Ionics*, 176 (2005) 2701.
34. L. P. Teo & M. H. Buraidah & A. F. M. Nor & S. R. Majid, *Ionics* DOI 10.1007/s11581-012-0667-2.
35. M.H. Buraidah, L.P. Teo, S.R. Majid, A.K. Arof, *Physica B* 404 (2009) 1373.
36. A.A Hendi, *Australian J. Basic and Applied Sci.*, 5 (2009) 380.
37. D.P Almond, A.R West, *Solid State Ionics*, 9&10 (1983) 277.

38. M. Vijayakumar, G. Hirankumar, M.S. Bhuvaneswari, S. Selvasekarapandian, *J. Power Sources* 117 (2003) 143.
39. T. Savitha a, S. Selvasekarapandian, C.S. Ramya, M.S. Bhuvaneswari ,G. Hirankumar, R. Baskaran, P.C. Angelo, *J. Power Sources* 157 (2006) 533.
40. A.M Abo El Ata, S.M Atia and T.M Meaz, *Solid State Sciences*, 6 (2004) 61.
41. Dev K. Mahato , Alo Dutta , T.P. Sinha, *Physica B*, 406 (2011) 2703.
42. N. A Hegab, A .E Bekheet, M .A Afifi, L. A Wahaba and H A Shehata, *J. Ovonic Res.*, 3 (2007) 71.
43. C.R Mariappan and G .Govindaraj, *Mater. Sci. Engin. B*, 94 (2002) 82.
44. E. G. El-Metwally, M. Fadel, A.M Shakra and M.A Afifi , *J. Optoelectronics and Advanced Mater.*, 10 (2008) 1320.